View metadata, citation and similar papers at core.ac.uk
brought to you by CORE
provided by ScholarWorks@UNIST

Electronic Supplementary Information

Hybrid Multilayer Thin Film Supercapacitor of Graphene Nanosheets with Polyaniline: Importance of Establishing Intimate Electronic Contact through Nanoscale Blending

*Taemin Lee, Taeyeong Yun, Byeongho Park, Bhawana Sharma, Hyun-Kon Song, and Byeong-Su Kim**

Interdisciplinary School of Green Energy and KIER-UNIST Advanced Center for Energy, Ulsan National Institute of Science and Technology (UNIST), Ulsan 689-798, Korea

bskim19@unist.ac.kr

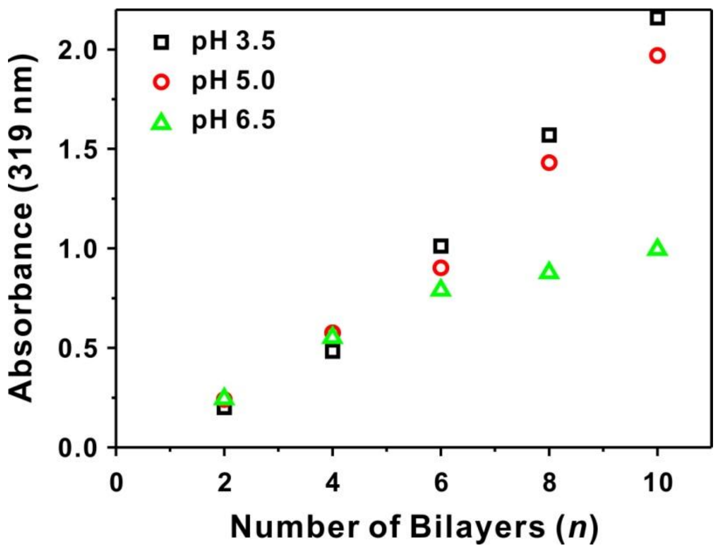

Fig. S1 Plot of the UV/vis absorption peak at 319 nm of PG_n multilayer film as a function of the number of bilayers constructed with varying pH of GO suspension at a fixed pH of PANi (pH 2.5).

Fig. S2 Representative photograph image of LbL-assembled hybrid electrodes of (left) PG_{10} (middle) PG_{10}-H, and (right) PG_{10}-HC.

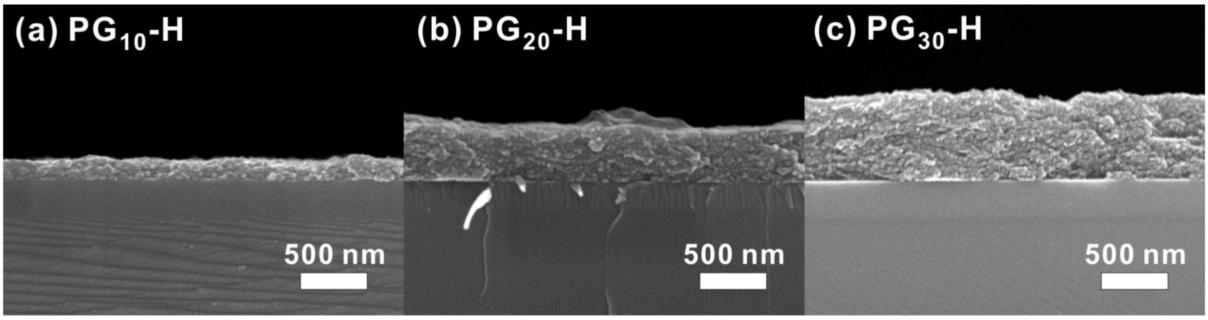

Fig. S3 Representative SEM images of PG_n-H multilayer films of different number of bilayers. (a) n = 10, (b) n = 20, and (c) n = 30.

Table S1 XPS peak assignments of deconvoluted C1s and N1s composition with relative percentage of each peak.

	Binding Energy (eV) / relative percentage (%)								
	C 1s						N 1s		
	C=C	C-C	C-N	C-O	C=O	O-C=O	=N-	-NH-	N^+
PG_{10}	284.37	285.1	285.8	286.63	287.95	289.89	398.21	399.37	401.09
	(48.32)	(14.96)	(4.37)	(19.71)	(10.43)	(2.21)	(10.53)	(48.85)	(40.62)
PG_{10}-H	284.38	285.08	285.84	286.67	287.87	289.23	398.22	399.5	401.09
	(57.37)	(12.89)	(10.7)	(7.1)	(7.31)	(4.63)	(9.68)	(58.2)	(27.11)
PG_{10}-HC	284.45	285.16	285.83	286.63	287.87	289.36	398.21	399.57	401.07
	(59.79)	(8.27)	(12.76)	(7.05)	(7.64)	(4.48)	(4.81)	(61.26)	(33.93)

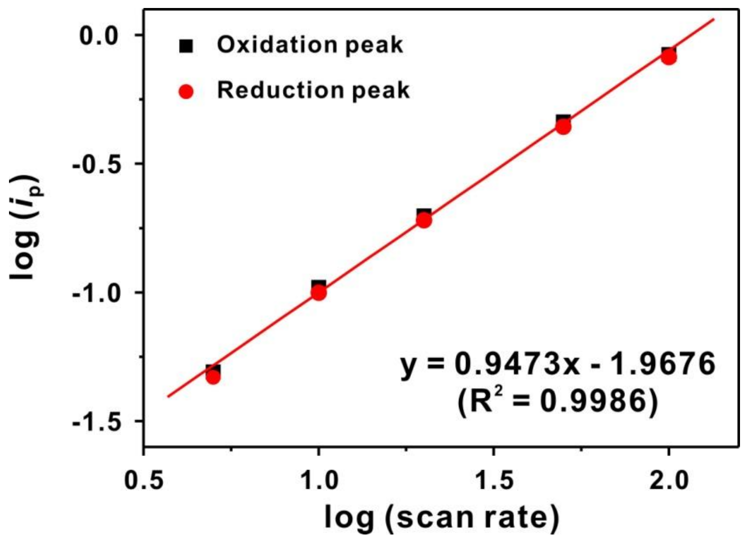

Fig. S4 Plot of the peak current density (mA cm^{-2}) *vs* potential scan rate (mV s^{-1}) of PG_{10}-H in an equi-span log-log scale. The slopes were estimated to be around 1.0 for both cases.

This journal is © The Royal Society of Chemistry 2012

Table S2 Specific capacitance values of hybrid PG_{10}, PG_{10}-H, PG_{10}-HC, and GG_{10}-H electrodes obtained from cyclic voltammograms and galvanostat charge/discharge experiments.

	Specific capacitance (F g^{-1}) (from cyclic voltammograms)				
	10 mV s^{-1}	20 mV s^{-1}	50 mV s^{-1}	100 mV s^{-1}	200 mV s^{-1}
PG_{10}	402.48	326.17	269.18	241.54	219.35
PG_{10}-H	489.04	400.13	349.92	323.76	304.76
PG_{10}-HC	240.13	180.53	135.01	116.85	103.54
GG_{10}-H	24.62	19.08	15.3	12.84	10.94

	Specific capacitance (F g^{-1}) (from charge/discharge curves)					
	0.5 A g^{-1}	1 A g^{-1}	1.5 A g^{-1}	2.0 A g^{-1}	2.5 A g^{-1}	3.0 A g^{-1}
PG_{10}	162.89	136.24	121.04	103.64	101.15	94.23
PG_{10}-H	375.15	218.43	163.92	129.92	124.65	116.46

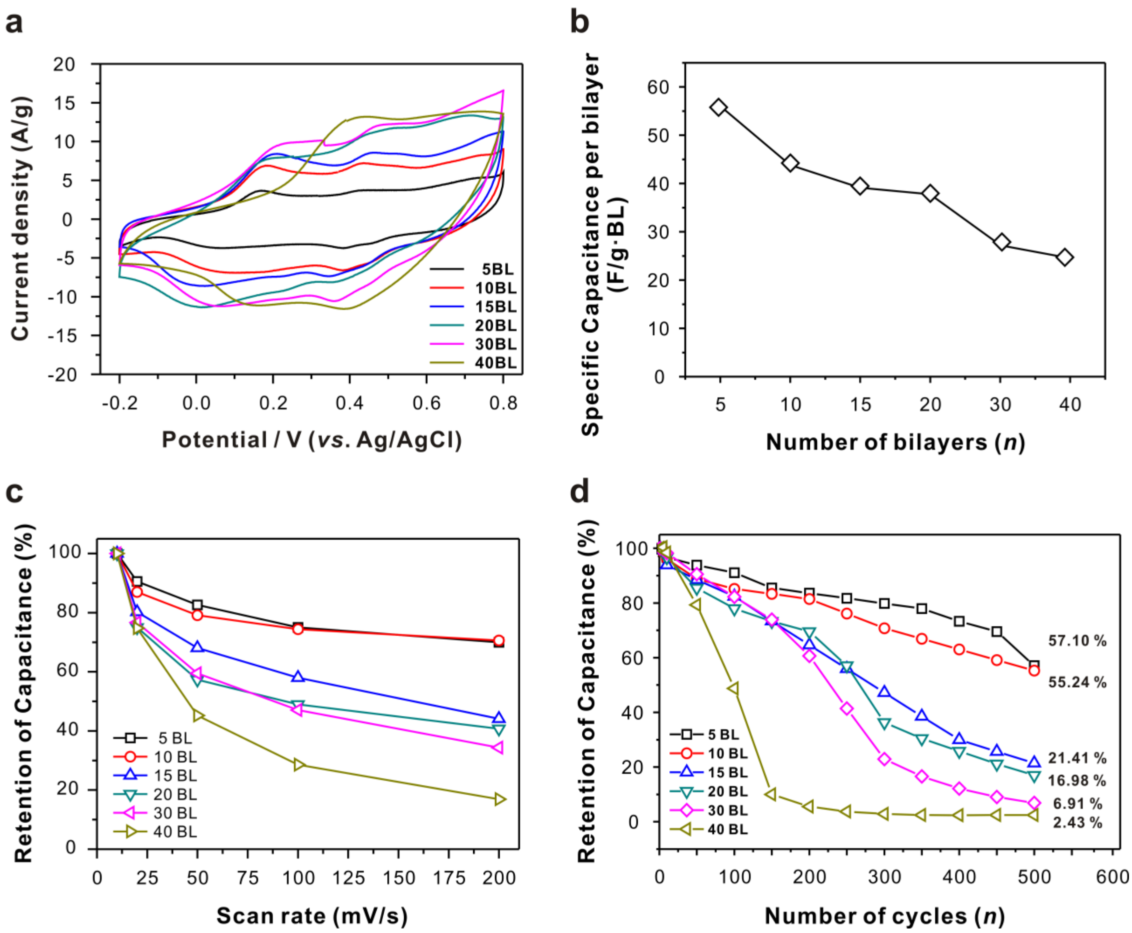

Fig. S5 Electrochemical performance of LbL-assembled PG_n–H multilayer films of different number of bilayers (n = 5, 10, 15, 20, 30, 40). (a) Cyclic voltammogram (CV) curves measured in a three-electrode system with a Ag/AgCl reference electrode in 1.0 M H_2SO_4 at a scan rate of 10 mV s^{-1}. (b) Plot of the specific capacitance per bilayer with respect to different numbers of bilayer. (c, d) Electrochemical stability of all PG_n–H multilayer films depending on (c) various scan rates from 10 to 200 mV s^{-1} and (d) number of cycles measured at a scan rate of 200 mV s^{-1}.

This journal is © The Royal Society of Chemistry 2012

Table S3 Specific capacitance values of PG$_n$–H (n = 5, 10, 15, 20, 30, 40) multilayer films of various number of bilayers obtained from cyclic voltammograms.

	Specific capacitance (F g^{-1}) (from cyclic voltammograms)				
BL	10 mV s^{-1}	20 mV s^{-1}	50 mV s^{-1}	100 mV s^{-1}	200 mV s^{-1}
PG_5-H	280.14	253.63	231.54	210.14	196.03
PG_{10}-H	489.04	400.13	349.92	323.76	304.76
PG_{15}-H	587.22	471.13	399.84	340.49	259.04
PG_{20}-H	755.06	566.64	432.68	369.89	307.53
PG_{30}-H	816.90	626.36	486.07	384.52	280.71
PG_{40}-H	980.51	733.40	443.51	280.41	165.72

Table S4 List of electrochemical capacitance values of various PANi-GO hybrid electrodes from recent literatures.

System	Specific Capacitance	Measurement Condition	Reference
Simple mixing	210 F g^{-1}	discharge current density at 0.3 A g^{-1}	*G. Shi et al., **ACS Nano** (2010)*[1]
In situ polymerization	260 F g^{-1}	discharge current density at 0.5 A g^{-1}	*J. Wu et al., **Chem. Mater.** (2010)*[2]
	555 F g^{-1}	discharge current density at 0.2 A g^{-1}	*Z, Wei et al., **ACS Nano** (2010)*[3]
	746 F g^{-1}	discharge current density at 0.2 A g^{-1}	*X. Wang et al., **ACS Appl. Mater. Interfaces** (2010)*[4]
	1046 F g^{-1}	CV Scan rate at 1 mV s^{-1}	*F. Wei et al., **Carbon** (2010)*[5]
	286 F g^{-1}	discharge current density at 0.3 A g^{-1}	*G. D. Fu et al., **Macromol. Rapid Commun.** (2011)*[6]
	250 F g^{-1}	CV Scan rate at 100 mV s^{-1}	*J.-B. Baek et al., **ACS Nano** (2012)*[7]
In situ electropolymerzation	233 F g^{-1}	CV Scan rate at 20 mV s^{-1}	*H.-M. Cheng et al., **ACS Nano** (2009)*[8]
	640 F g^{-1}	discharge current density at 0.1 A g^{-1}	*W. Huang et al., **Adv. Funct. Mater.** (2011)*[9]
	970 F g^{-1}	discharge current density at 2.5 A g^{-1}	*T. Cao et al., **Adv. Funct. Mater.** (2012)*[10]

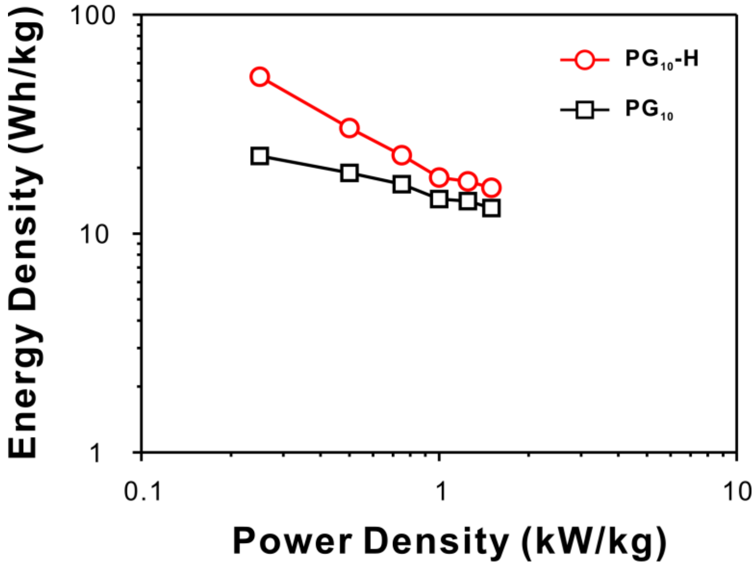

Fig. S6 Ragone plot of the LbL-assembled hybrid PG_{10} (black-line) and PG_{10}-H (red-line) supercapacitor electrodes measured at different discharge current density from 0.5 to 3 A g^{-1}.

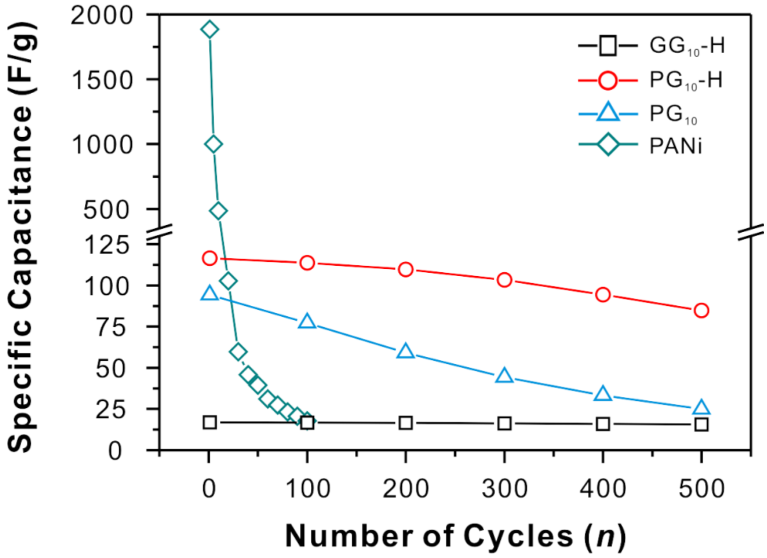

Fig. S7 Comparison of cycling stability of all samples at a high discharge current density of 3 A g^{-1}. Electropolymerized pure PANi film was used for comparison.

References

1. Q. Wu, Y. Xu, Z. Yao, A. Liu, G. Shi, *ACS Nano,* 2010, **4**, 1963-1970.
2. K. Zhang, L. L. Zhang, X. S. Zhao, J. Wu, *Chem. Mater.*, 2010, **22**, 1392-1401.
3. J. Xu, K. Wang, S.-Z. Zu, B.-H. Han, Z. Wei, *ACS Nano*, 2010, **4**, 5019-5026.
4. H. Wang, Q. Hao, X. Yang, L. Lu, X. Wang, *ACS Appl. Mater. Interfaces*, 2010, **2**, 821-828.
5. J. Yan, T. Wei, B. Shao, Z. J. Fan, W. Z. Qian, M. L. Zhang, F. Wei, *Carbon*, 2010, **48**, 487-493.
6. L. Q. Xu, Y. L. Liu, K.-G. Neoh, E.-T. Kang, G. D. Fu, *Macromol. Rapid Commun.*, 2011, **32**, 684-688.
7. N. A. Kumar, H.-J. Choi, Y. R. Shin, D. W. Chang, L. Dai, J.-B. Baek, *ACS Nano*, 2012, **6**, 1715-1723.
8. D.-W. Wang, F. Li, J. Zhao, W. Ren, Z.-G. Chen, J. Tan, Z.-S. Wu, I. Gentle, G. Q. Lu, H.-M. Cheng, *ACS Nano*, 2009, **3**, 1745-1752.
9. X. M. Feng, R. M. Li, Y. W. Ma, R. F. Chen, N. E. Shi, Q. L. Fan, W. Huang, *Adv. Funct. Mater.* 2011, **21**, 2989-2996.
10. M. Xue, F. Li, J. Zhu, H. Song, M. Zhang, T. Cao, *Adv. Funct. Mater.* 2012, **22**, 1284-1290.